

Supplementary Information

Synthesis and Catalytic Activity of Pluronic Stabilized Silver-Gold Bimetallic Nanoparticles

*Megan S. Holden*¹, *Kevin E. Nick*², *Mia Hall*³, *Jamie R. Milligan*⁴, *Qiao Chen*⁵, and *Christopher C. Perry*^{*1}

¹Department of Basic Sciences, School of Medicine, Loma Linda University, Loma Linda, CA

92350

²Department of Earth and Biological Sciences, School of Medicine, Loma Linda University,

Loma Linda, CA 92350

³Elizabeth City State University, 1704 Weeksville Rd, Elizabeth City, NC 27909

⁴Department of Radiology, University of California, San Diego, 9500 Gilman Drive, La Jolla,

CA 92093

⁵Chemistry Department, School of Life Sciences, Sussex University, Brighton, BN1 9QJ, UK

*¹ Corresponding author : E-mail chperry@llu.edu; Phone: 1-909-558-9702

S1. Determination of Catalytic Efficiency

For a first-order reaction, the rate is written as:

$$-\frac{dC}{dt} = k_{app}C(t) = k_1 \cdot S \cdot C(t) \quad (1)$$

where the apparent rate constant k_{app} is proportional to the total surface area per unit volume of the solution, S , available from the nanoparticles.¹ The terms $C(t)$ and k_1 represent 4-nitrophenol concentration and the rate constant normalized to S , respectively. We use the turnover frequency (TOF) with dimensions of time⁻¹ to quantify catalytic efficiency. The TOF at a specified temperature is defined as the derivative of the number of turnovers (N) with respect to the time (t),² and is equal to k_{app} at the saturation limit for first-order reactions:^{2a}

$$TOF = -\frac{dN}{dt} = k_1 \cdot \frac{[C]}{c^0} = TOF^\circ \cdot \frac{[C]}{c^0} \quad (2)$$

TOF° is defined as the specific TOF at a concentration of $[C]$ equal 1 M (c^0 is the standard concentration of 1 M). Under our conditions, the derivatives of absorbance and concentration are

proportional to each other, hence $\frac{\Delta A}{\Delta t} \propto \frac{\Delta N}{\Delta t}$. This definition avoids the ambiguities of the alternative definitions found in the literature and allows for meaningful comparisons among catalytic systems.² To standardize the conditions, TOF is expressed as a “standard turnover frequency” where the reactant and products are 1 M and temperature set at 273.15 K according to STP conditions

$$TOF^\circ = TOF(T) \cdot \frac{T^0}{T} \cdot e^{\frac{\delta E}{R} \cdot \left(\frac{1}{T^0} - \frac{1}{T} \right)} \quad (3)$$

Where R is the gas constant and δE is the activation energy determined from Arrhenius plots.

Furthermore, when is TOF normalized to S , it has units $Lm^{-2} s^{-1}$.

S2. Determination of Surface to volume ratios from Langmuir adsorption isotherms

Adsorption Isotherms and Langmuir Plots

The surface coverage of the NPs was determined using a modified protocol described by Mahmoud and co-workers.³ A stock solution of ≈ 0.2 mM 4-nitrothiophenol (4-NTP) was prepared in DI water and the pH was adjusted to ≈ 6.5 using 0.1 M sodium hydroxide. The amount of 4-NTP adsorbed on the surface of the NPs was determined from optical measurements using our measured extinction coefficient (11637 ± 133 L mol⁻¹ cm⁻¹). The resulting solution was yellow in color and had an optical absorption peak at 410 nm. In 11 microcentrifuge tubes, 50 μ L of as-prepared NP solutions were added to 4-NTP to achieve final 4-NTP concentrations ranging from 0.0 – 10×10^{-5} M in a 1 mL final volume. The solutions were shaken in the dark by a mechanical shaker for 24 h and centrifuged (17,900 g for 30 minutes) to remove the NPs. The supernatants (300 μ L) were then transferred to a 96-well plate and the absorbance measured at 410 nm using a 96-well plate reader where the absorbance path-length correction was 1.16. The equilibrium concentration was calculated from the adsorption peak intensity of the supernatant. The concentration of adsorbed 4-NTP was determined from the difference between in absorbance intensities of 4-NTP with and without NPs.

The surface-to-volume ratios were determined from Langmuir plots, which gives the relationship between the concentrations of adsorbed 4-NTP and the equilibrium concentration of 4-NTP remaining after the adsorption process. The Langmuir equation is:

$$C_{ads} = \frac{K \cdot C_m \cdot C_{eq}}{1 + K \cdot C_{eq}} \quad (1a)$$

where C_{ads} and C_{eq} are the concentrations of adsorbed and solution 4-NTP, K is the binding constant, and C_m is the monolayer concentration. After linearizing the Langmuir equation, the

slope of the $\frac{C_{eq}}{C_{ads}}$ vs C_{eq} will give the reciprocal of the concentration of adsorbed NPs.

$$\frac{C_{eq}}{C_{ads}} = \frac{1}{K \cdot C_m} + \frac{C_{eq}}{C_m} \quad (1b)$$

Thus, the surface-to-volume ratio will be:

$$S/V = 1/\text{slope} \times N_A \times 1.87 \times 10^{-19} \text{ m}^2 \quad (2)$$

Where, N_A is Avogadro's number and $1.87 \times 10^{-19} \text{ m}^2$ is the average surface of each 4-NTP molecule.³ The validity of this approach was verified by the similar values within factor of 2 of S/V ratios obtained from the isotherm adsorptions ($\approx 0.5 \text{ m}^2/\text{L}$) and estimations based upon Ag or Au NP sizes ($\sim 22\text{--}25 \text{ nm}$) ($S/V = \pi D^2 \times \text{NP concentration} (\sim 0.1 \text{ mM}) \times N_A \approx 0.2 \text{ m}^2/\text{L}$).

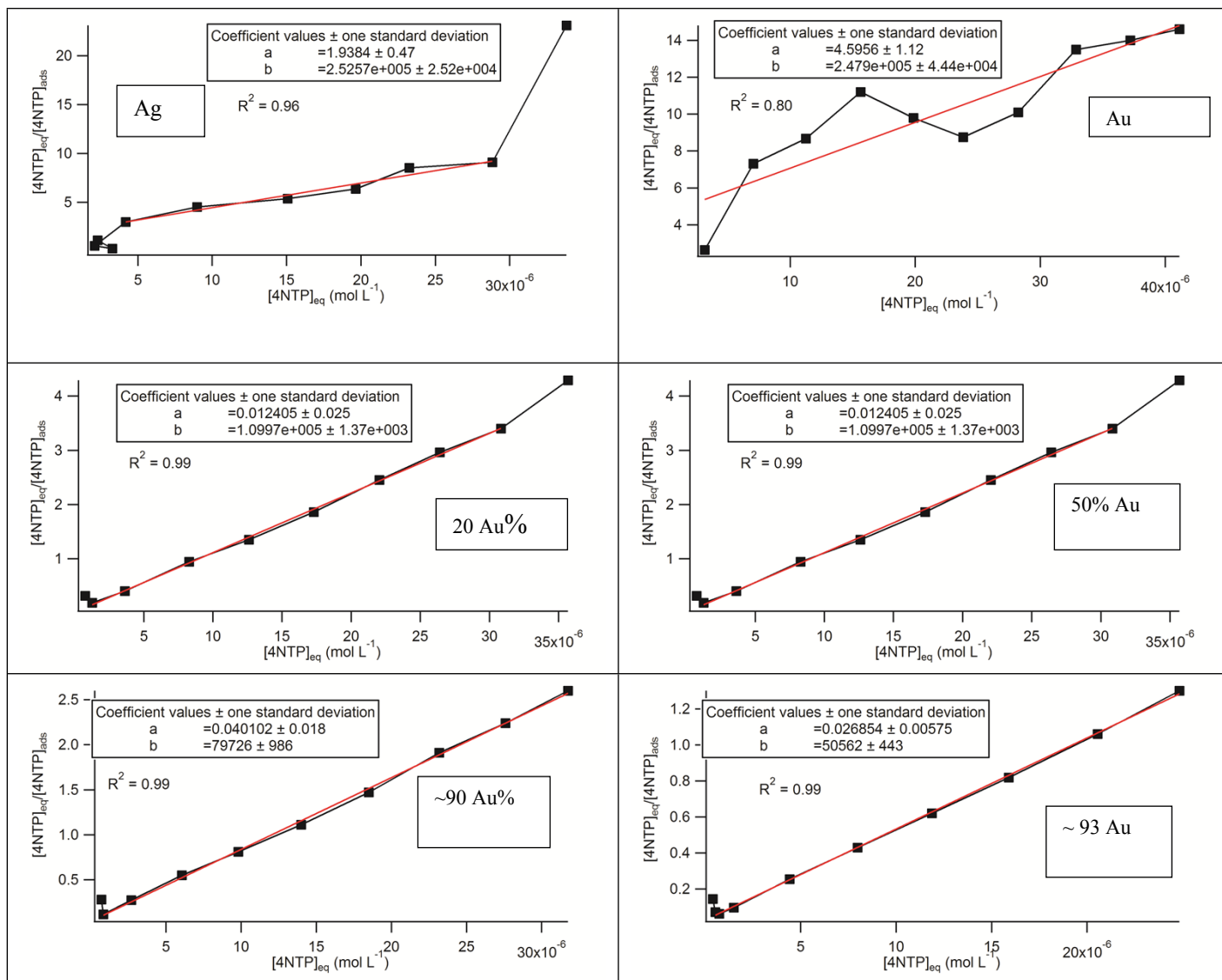


Figure S1. Langmuir plots of the $\frac{C_{ads}}{C_{eq}}$ vs C_{eq} where the reciprocal of the slope is average the monolayer 4-NTP concentration on the NP. The concentrations were determined from absorbance measurements from a 96-well plate reader and a total volume of 300 μ L. The concentration was determined using our measured extinction coefficient (11637 ± 133 L mol⁻¹ cm⁻¹), which was multiplied by a path-length correction factor of 1.16. The top panel are plots of Ag and Au NPs and the second and third panels are the bimetallic Ag-Au NPs of increasing Au percent. The middle panel are representative plots of BNPs comprising 20 and 50% Au, and the bottom panel are plots of BNPs comprising ~90 – 95 % Au.

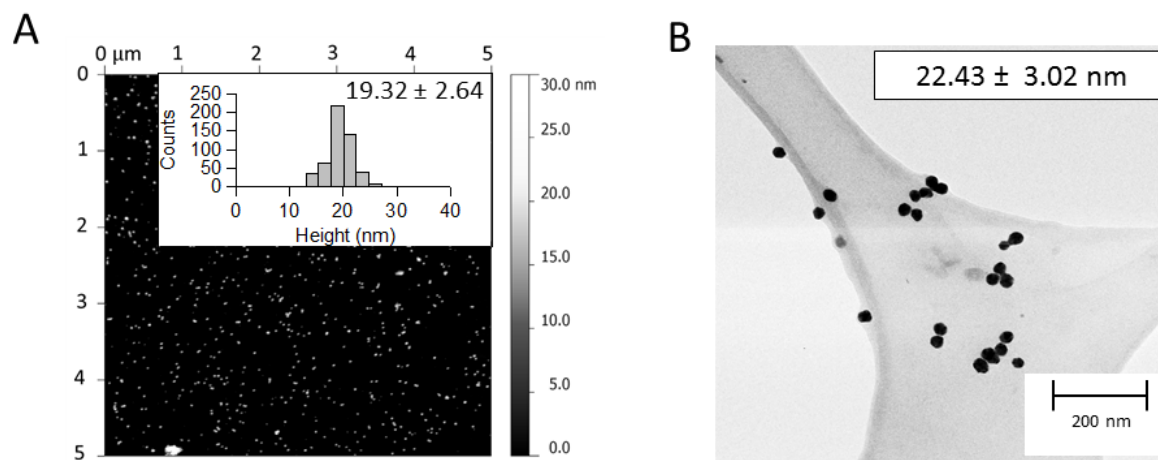


Figure S2. (A) AFM image and NP height distribution for Ag NPs. (B) TEM image and mean diameter of Ag NPs.

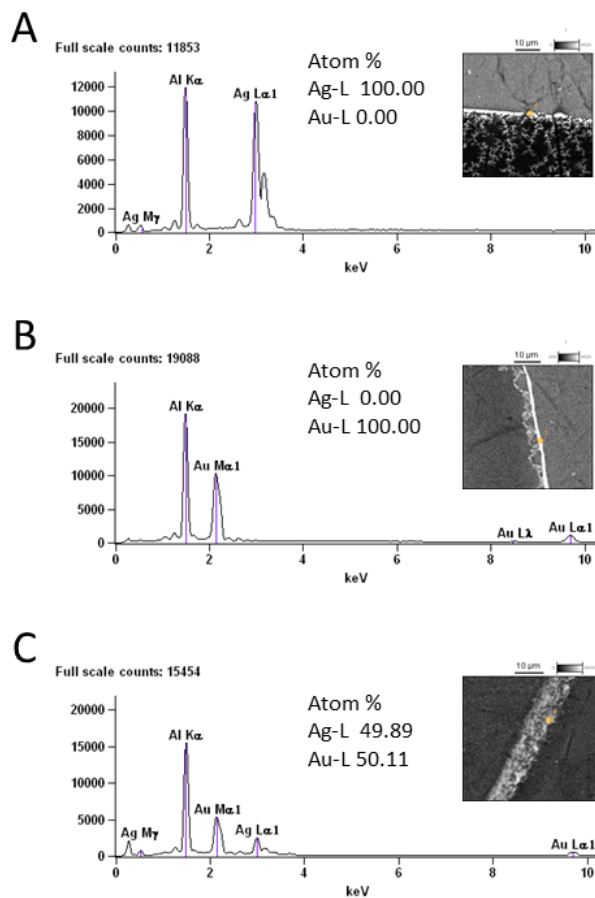


Figure S3. Typical EDX analysis data sets for NPs. Data are elementary composition table (calculated exclusively by fitting silver and gold contributions), SEM image of the analyzed region, EDX spectrum for (A) Ag NPs, (B) Au NPs, and (C) Ag-Au NPs.

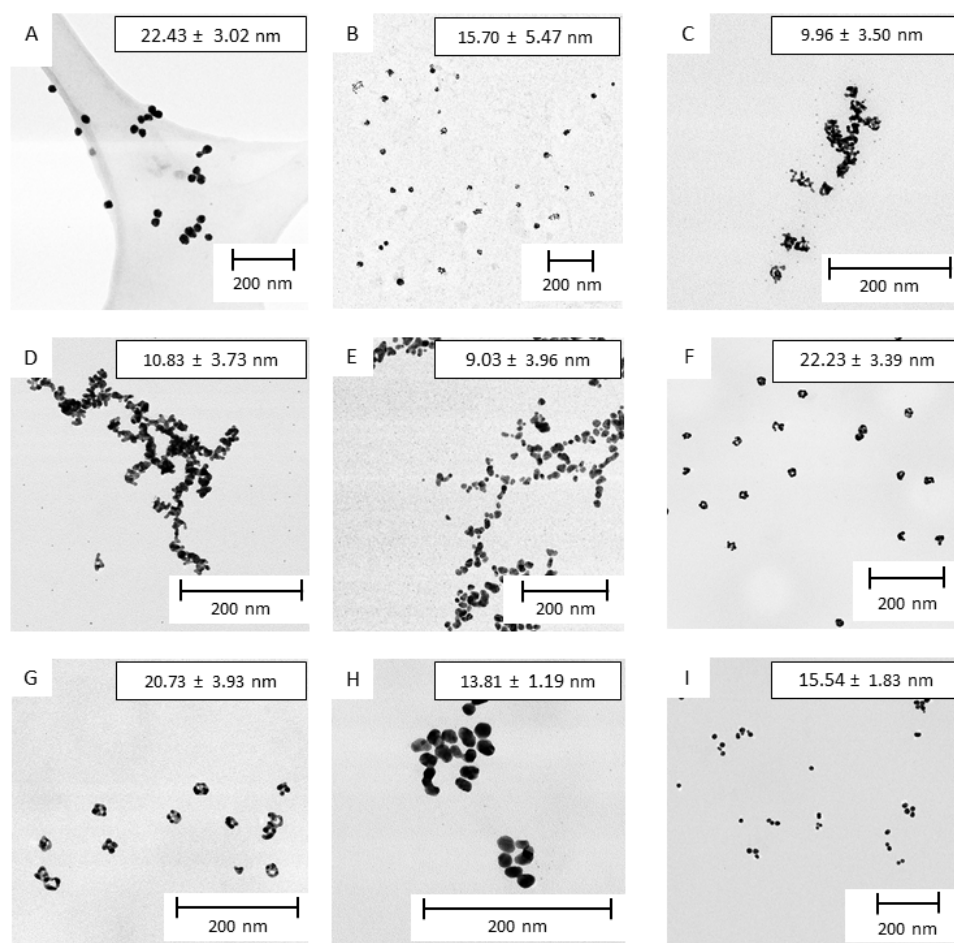


Figure S4. TEM images of (A) Ag (top left) and Ag-Au nanoparticles prepared at 25°C after (B) 2×10^{-4} M ($\approx 20\%$ Au), (C) 4×10^{-4} M ($\approx 40\%$ Au), (D) 6×10^{-4} M ($\approx 60\%$ Au), and (E) 8×10^{-4} M ($\approx 75\%$ Au) of H[AuCl₄] were added. Bottom panel are images of NPs prepared at 100°C after (F) 2×10^{-4} M ($\approx 20\%$ Au), (G) 4×10^{-4} M ($\approx 50\%$ Au), and (H) 6×10^{-4} M ($\approx 90\%$ Au), and (I) 8×10^{-4} M ($\approx 93\%$ Au) of H[AuCl₄] were added.

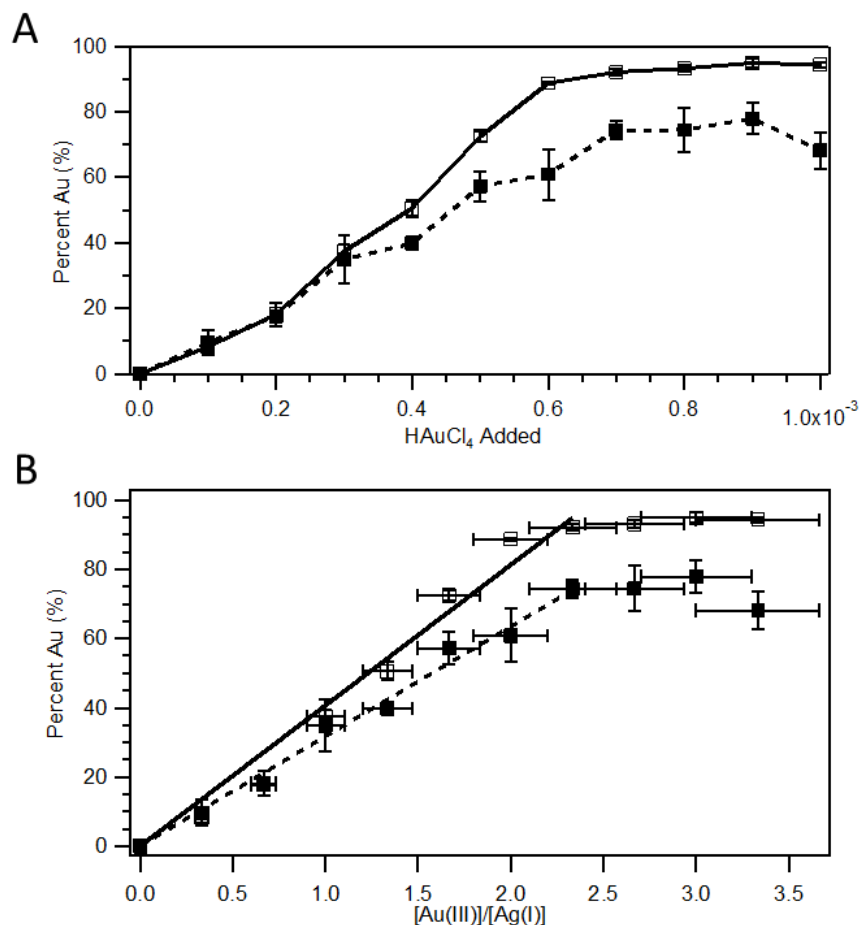


Figure S5. Elemental Ag-Au determination by the EDX. The total Ag atom concentration in the Ag seed nanoparticles is $\approx 3 \times 10^{-4}$ M. (A) Variation in the percent Au composition against H[AuCl₄] added to Ag nanoparticles (OD ≈ 12 ; ≈ 1 nm) at room temperature (solid squares) and heated to 100 °C (open squares). The solid and dashed lines are visual guides. (B) Variation in percent Au against initial Au(III)/Ag(I) ratios at room temperature (solid squares) and heated to 100 °C (open squares). There is a linear relationship between Au composition and the Au(III)/Ag(I) ratios at room temperature (solid line) and at 100 °C (dotted line). The values are mean \pm SD.

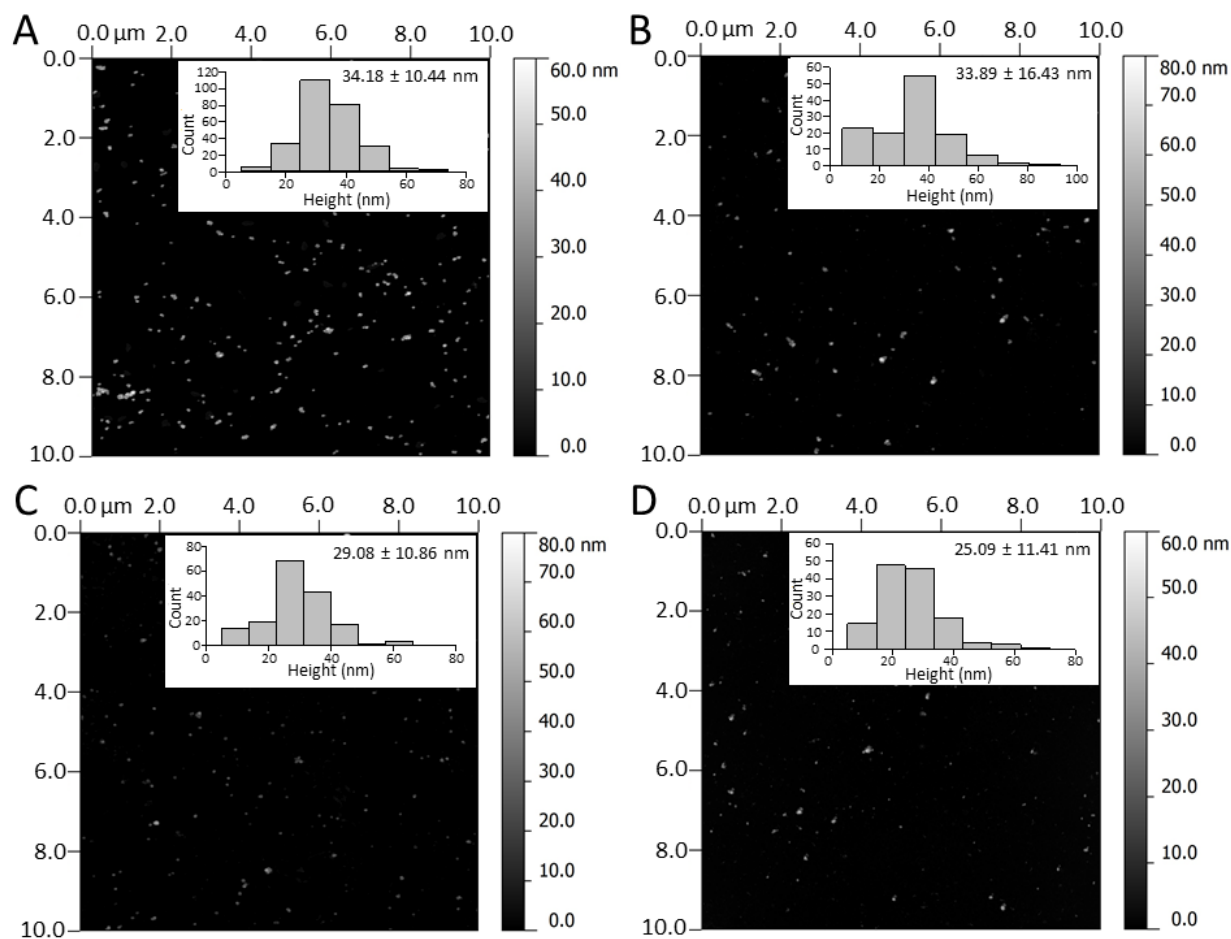


Figure S6. AFM height images. The nanoparticles were prepared by adding HAuCl_4 (1 to 8 μL ; 0.1 M) to 1 mL of ≈ 1 nM ($\text{OD} \approx 12$) 25 nm Ag nanoparticles at 100°C . Images taken after (A) 2×10^{-4} M ($\approx 20\%$ Au), (B) 4×10^{-4} M ($\approx 50\%$ Au), and (C) 6×10^{-4} M ($\approx 90\%$ Au), and (D) 8×10^{-4} M ($\approx 93\%$ Au) of HAuCl_4 were added.

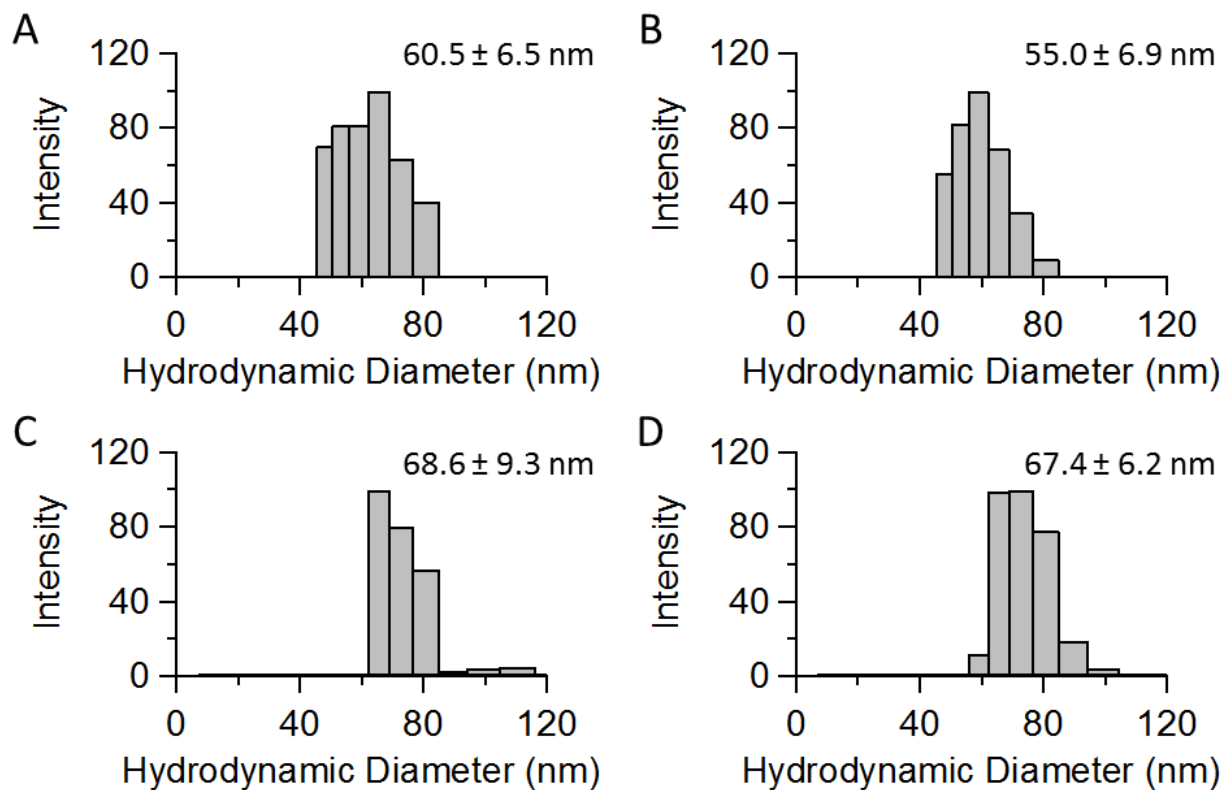


Figure S7. Intensity weighted DLS of Ag-Au NPs. The nanoparticles were prepared by adding H_{AuCl}₄ (1 to 8 μ L; 0.1 M) to 1 mL of \approx 1 nM (OD \approx 12) 25 nm Ag nanoparticles at 100°C. DLS after (A) 2×10^{-4} M (\approx 20% Au;), (B) 4×10^{-4} M (\approx 50% Au), and (C) 6×10^{-4} M (\approx 90% Au), and (D) 8×10^{-4} M (\approx 93% Au) of H_{AuCl}₄ were added.

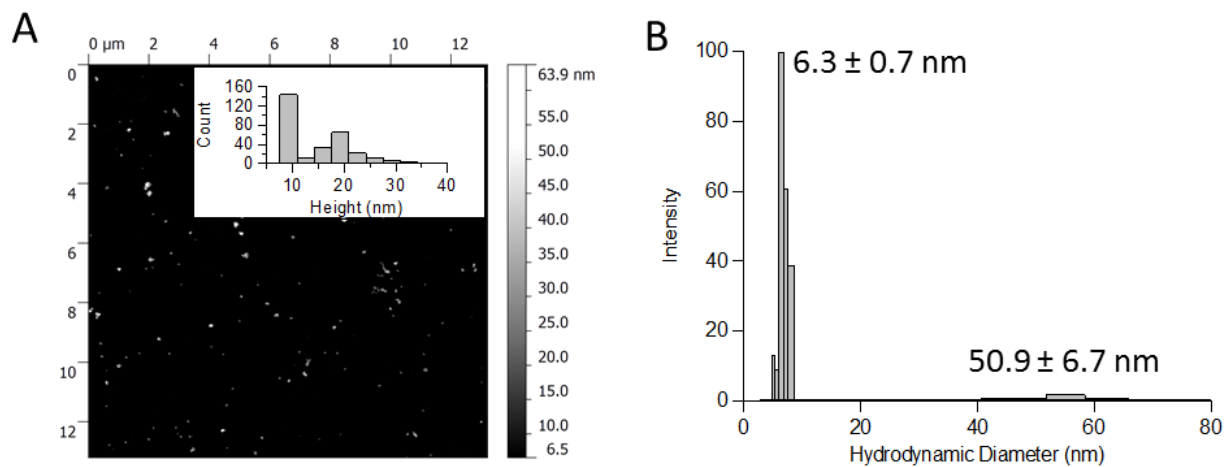


Figure S8. (A) AFM height and (B) intensity weighted DLS distributions of Au:Ag ratio ~ 3.5 NPs prepared from Ag NP seeds at 100°C . The nanoparticles were prepared by adding HAuCl_4 ($10\ \mu\text{L}$; $0.1\ \text{M}$) to $1\ \text{mL}$ of $\approx 1\ \text{nM}$ ($\text{OD} \approx 12$) $25\ \text{nm}$ Ag nanoparticles at 100°C . A bimodal distribution of smaller and larger NPs is evident upon the addition large molar excess of HAuCl_4 .

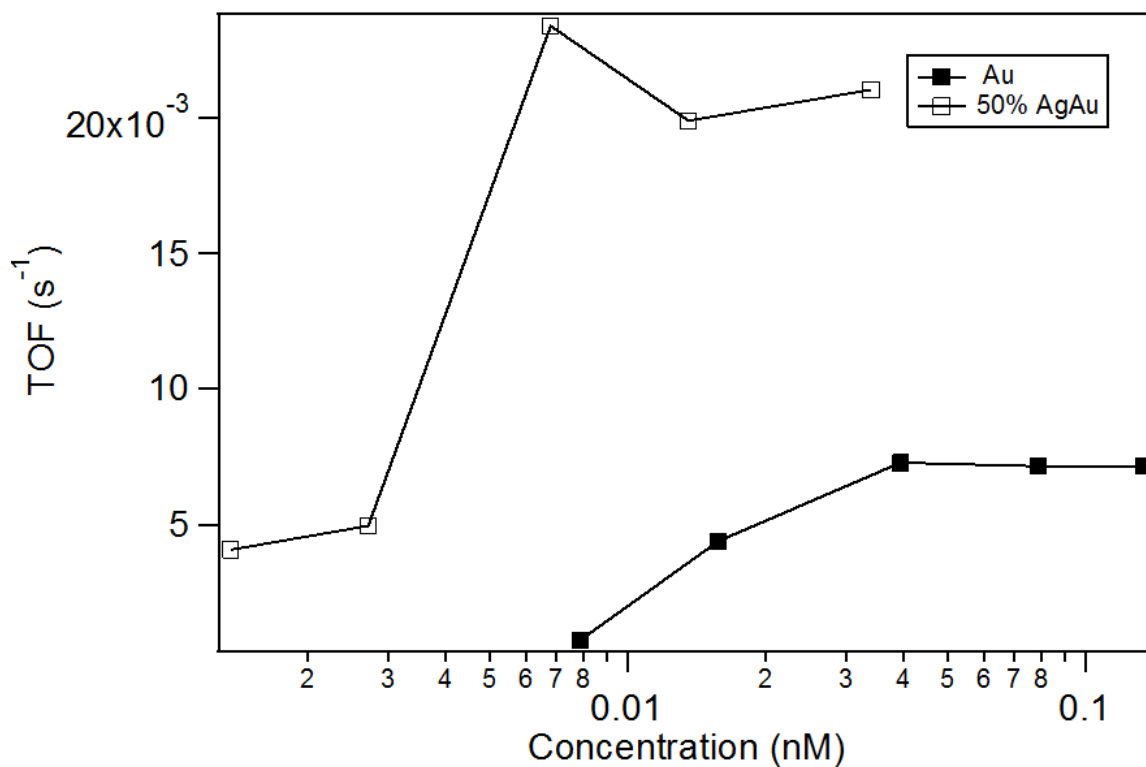


Figure S9. Determination of the saturation limits of NP catalysts. Plot of TOFs at room temperature against concentration of NPs in the reduction of 4-nitrophenol. Experimental TOFs to determine rate constants were measured above the saturation limits of the Au and Ag-Au NP catalysts at 0.134 and 0.034 mM, respectively. The citrated Au NPs (~ 25 nm) were coated in F127 by centrifuging (10,000×g, 20 minutes) followed by suspension in ≈ 2% (w/v) aqueous Pluronic F127. The bimetallic nanoparticles were prepared by adding HAuCl₄ (4 μL; 0.1 M) to 1 mL of ≈ 1 nM (OD ≈ 12) 25 nm Ag nanoparticles at 100°C.

REFERENCES

1. (a) Wunder, S.; Lu, Y.; Albrecht, M.; Ballauff, M., Catalytic Activity of Faceted Gold Nanoparticles Studied by a Model Reaction: Evidence for Substrate-Induced Surface Restructuring. *ACS Catal.* **2011**, *1* (8), 908-916; (b) Wunder, S.; Polzer, F.; Lu, Y.; Mei, Y.; Ballauff, M., Kinetic Analysis of Catalytic Reduction of 4-Nitrophenol by Metallic Nanoparticles Immobilized in Spherical Polyelectrolyte Brushes. *J. Phys. Chem. C* **2010**, *114*, 8814–8820.
2. (a) Kozuch, S.; Martin, J. M. L., “Turning Over” Definitions in Catalytic Cycles. *ACS Catal.* **2012**, *2* (12), 2787-2794; (b) Umpierre, A. P.; de Jesús, E.; Dupont, J., Turnover Numbers and Soluble Metal Nanoparticles. *ChemCatChem* **2011**, *3* (9), 1413-1418.
3. Mahmoud, M. A.; Garlyyev, B.; El-Sayed, M. A., Determining the Mechanism of Solution Metallic Nanocatalysis with Solid and Hollow Nanoparticles: Homogeneous or Heterogeneous. *J. Phys. Chem. C* **2013**, *117* (42), 21886-21893.